

**Role of transitional levels in  $^{237}\text{Np}(\gamma, f)$ : Perspectives for studying highly deformed systems**J. D. T. Arruda-Neto,<sup>1,6</sup> J. Mesa,<sup>2</sup> F. Garcia,<sup>3</sup> O. Rodriguez,<sup>1,4</sup> L. P. Geraldo,<sup>5,7</sup> C. Garcia,<sup>4</sup> T. E. Rodrigues,<sup>1</sup> K. Shtejer,<sup>1</sup> R. Semmler,<sup>5</sup> and F. Guzmán<sup>4</sup><sup>1</sup>*Instituto de Física, Universidade de São Paulo, São Paulo, SP, Brazil*<sup>2</sup>*Instituto de Biociências, Universidade Estadual de São Paulo, Botucatu, SP, Brazil*<sup>3</sup>*Universidade Estadual de Santa Cruz, Ilhéus, BA, Brazil*<sup>4</sup>*Instituto Superior de Tecnologías y Ciencias Aplicadas, Havana, Cuba*<sup>5</sup>*Instituto de Pesquisas Energéticas e Nucleares/IPEN, São Paulo, SP, Brazil*<sup>6</sup>*Universidade de Santo Amaro/UNISA, São Paulo, SP, Brazil*<sup>7</sup>*Universidade Católica de Santos/UNISANTOS, Santos, SP, Brazil*

(Received 19 November 2004; revised manuscript received 13 April 2006; published 21 September 2006)

The transition levels at the top of the two  $^{237}\text{Np}$  fission barriers were obtained for the first time by means of the so-called semimicroscopic combined method, which we have developed and implemented. To overcome the difficulties in dealing with large nuclear deformations, we used our developed BARRIER code, which calculates single-particle spectra in a deformed Woods-Saxon potential using a coordinate system based on Cassini ovoids as nuclear shape parametrization. The results enabled us to describe the experimentally observed near-barrier photofission cross-section structures for  $^{237}\text{Np}$ , as well as a subbarrier shelf, the latter being consistently interpreted in terms of the accumulation of levels at the top of the inner and outer double fission barrier of  $^{237}\text{Np}$ .

DOI: [10.1103/PhysRevC.74.034324](https://doi.org/10.1103/PhysRevC.74.034324)

PACS number(s): 25.85.Jg, 21.60.-n

**I. INTRODUCTION**

One of the most interesting aspects of research on nuclear structure is the study of superdeformed and the search for hyperdeformed nuclei. In this regard, the fission reaction channel offers excellent possibilities. For example, sharp transmission resonances were observed in the fission reaction  $^{235}\text{U}(d, pf)^{236}\text{U}$  and interpreted as being hyperdeformed rotational bands lying in the third well of the fission barrier [1].

The investigation of low-energy fission processes provides key information on transition levels at the top of multistructured fission barriers and on quasistationary levels at their minima. In fact, spectroscopy of the second minimum has been attempted with success [2,3], as well as the efforts toward the delineation of a possible third minimum [4,5]. For odd- $N$  and/or odd- $Z$  nuclei, however, there is a major experimental shortcoming: photofission angular distributions are expected to be isotropic or nearly isotropic at energies somewhat above the barrier [2,4,6]. This fact prevents the unambiguous identification of quasistationary levels at the second minimum and of transition levels. Guesses about the nature of these levels are made only through the observation of the so-called *cross section irregularities* (shelves and structures) [4,7].

The cross section irregularities for subbarrier fission could also be associated with resonant penetration of the barrier. At energies above (but close to) the barrier, structures could be originated from the fission and neutron emission competing channels. However, the most interesting physics is contained in the cross-section irregularities caused by the transition spectrum structure, but the observation of low-energy structures in the fission cross section of odd heavy nuclei, or at least for odd- $Z$  nuclei, has been discarded by means of both experimental and theoretical arguments related to the absence of pairing gap of levels and the high level densities for these nuclei at low energies [8–10].

**II. A CASE STUDY:  $^{237}\text{Np}(\gamma, f)$** 

In spite of these difficulties we have decided to investigate  $^{237}\text{Np}$ , because of the following distinct characteristics:

(i) The neutron evaporation threshold is  $B_n \approx 6.6$  MeV, whereas its highest fission barrier is  $\sim 5.7$  MeV [11]. In this sense, all possible cross-section structures showing up at photon energies  $\omega \leq 6.6$  MeV cannot be associated with fission/neutron-emission competition.

(ii) A wide structure ( $\Delta W \approx 0.4$  MeV) around 5.7–5.8 MeV has been systematically observed in the photofission cross section [10,12].

(iii) such “unexpected” experimental finding for  $^{237}\text{Np}$  has been tentatively attributed either to the fission process itself [12,13] or to the photonuclear process [10].

(iv) In the detailed  $^{237}\text{Np}(\gamma, f)$  study of Soldatov *et al.* [10], the fission nature of the 5.7–5.8 MeV structure was ruled out, based on the argument that the fission probability of  $^{237}\text{Np}$  measured with other projectiles, as, e.g., in the reaction  $^{236}\text{U}(^3\text{He}, df)$  [8,9], shows no “irregularity” in this energy region.

(v) It has been suggested, however, in this same  $^{237}\text{Np}(\gamma, f)$  study [10], that the observed cross-section structure is a manifestation of a resonance-like structure in the photonuclear process, the so-called 5.5 MeV anomaly [14].

(vi) More recently, finally, a very high resolution cross-section measurement of  $^{237}\text{Np}(\gamma, f)$  revealed two structures at  $\sim 5.7$  and  $\sim 6$  MeV [15].

In fact, we measured the  $^{237}\text{Np}$  photofission cross section in the energy interval 5.27–10.83 MeV, using  $\gamma$ -ray spectra produced by thermal neutron capture [15]. As shown in Fig. 1, two structures show up clearly at  $\sim 5.7$  and  $\sim 6.0$  MeV and a shelf around 5.3 MeV. We show in Fig. 2 our results in the energy interval 5–7 MeV, together with other results available in the literature obtained with different techniques as

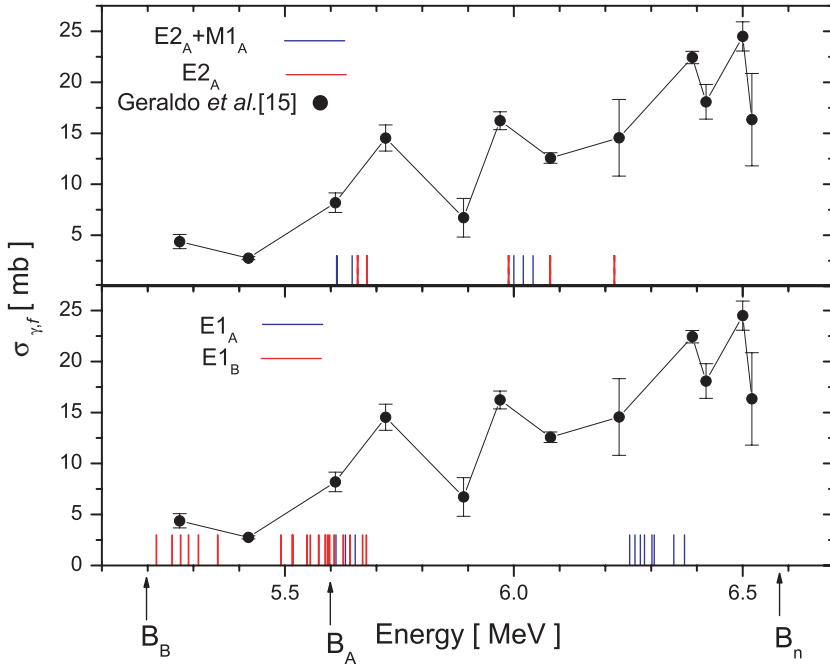


FIG. 1. (Color online) Photofission cross section of  $^{237}\text{Np}$  (data points) as function of the photon energy. The lines joining the data points are only to guide the eyes. Our results for the transition-nucleus levels are depicted as well. The subscripts  $A$  and  $B$  refer to the inner and outer fission barriers, respectively. Other details are in the text.

Bremsstrahlung photon beams [12] and photons produced by positron annihilation in flight [16]. Good overall agreement is verified in the whole energy interval. It is worth remembering that the  $\gamma$ s produced by thermal neutron capture have much higher energy resolution (only a few eV), as compared with other techniques.

### III. THEORETICAL APPROACH AND CALCULATIONS

In this article, detailed calculations are reported and several important points are discussed. Our main concern is to obtain from theory a complete description for the experimentally observed  $^{237}\text{Np}(\gamma, f)$  structures below  $B_n$ , as well as to address most of the issues commented above. The core of our approach

is to link for the first time the cross-section structures to transitional-state *clusters* on the top of the double-humped fission barriers. For the even-odd nucleus  $^{237}\text{Np}$ , which is strongly deformed at the saddle point, quasiparticle states (and rotational bands built on these quasiparticle states) will be calculated within the framework of an improved version of our method as described below.

Actually, the present calculations represent an application of our semimicroscopic combined method [17–19] developed for the description of fissionlike properties, which are strongly associated with single-particle effects in the vicinity and even beyond the saddle point. Thus, our approach strongly depends on accurate calculations of single-particle states for very deformed shapes. In this regard, it is necessary to achieve

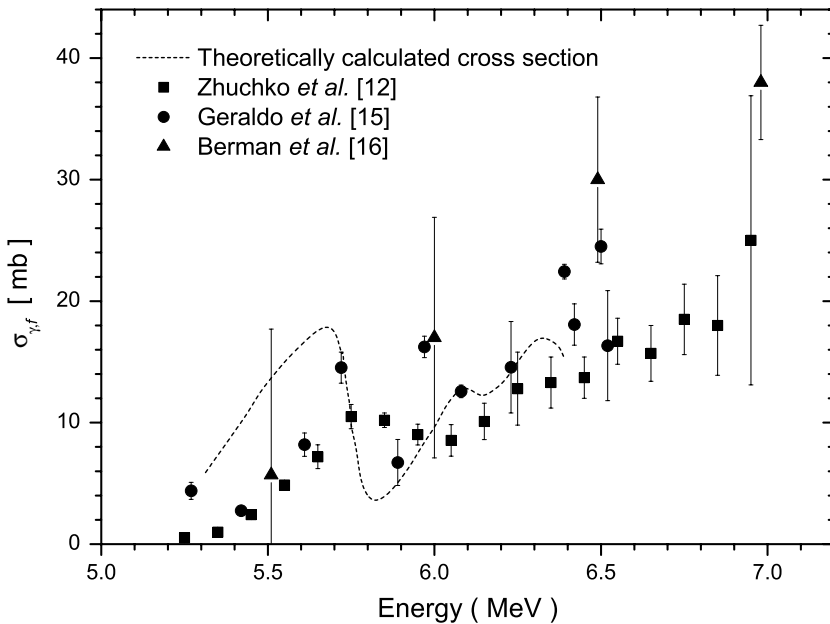


FIG. 2. Photofission cross section of  $^{237}\text{Np}$  measured by three different techniques: neutron-capture  $\gamma$  rays [15], Bremsstrahlung [12], positron annihilation in flight [16], and theoretically calculated photofission cross section (this work).

a consistent knowledge of such important ingredients. Previous works have shown several stringent tests demonstrating the excellent accuracy of the calculations, as, e.g., (a) the reproduction of the experimentally obtained spin, parity, and energies of the rotational band built on the  $8\text{-}\mu\text{s}$  isomeric state in  $^{239}\text{Pu}$  (spectroscopy of the second minimum; see Fig. 8 in Ref. [2] or Fig. 3(d) in Ref. [3]), (b) the full interpretation of the  $^{239}\text{Pu}$  photofission angular distributions (Fig. 9 and Table II in Ref. [2]), and (c) the detailed calculation of the  $^{233}\text{Pa}(n, f)$  cross section (see Fig. 1 in Ref. [17]).

We observe that the spectrum of transitional states of fissioning nuclei is similar to the spectrum of stable nuclei at equilibrium deformation. The nature of these states is collective (vibration and rotation) and quasiparticle. For some heavy nuclei, the majority of low-lying states (up to  $\sim 1$  MeV) are  $\gamma$  and octupole vibrations. However, for odd heavy deformed nuclei the relative contribution of these states is small, because of the great number of quasiparticle states at these excitation energies. Then, rotational states are introduced by the building up of a rotational band on each quasiparticle state. The calculation of the spectrum of quasiparticle states is not a simple task, because it requires a good knowledge of the mean field and of the residual interactions. In this sense, the calculation of low-lying quasiparticle states can be performed via the BCS model, which takes into account the main part of the residual interactions [18,19].

More specifically, we have calculated the transition levels of  $^{237}\text{Np}$ , where we used the so-called semimicroscopic combined method implemented in the DENCOM code [18,19]. The method uses the quantum statistical model proposed by Decowski *et al.* [20], which takes into account shell and pairing effects calculated in the framework of the BCS model. However, at low excitation energies, level-density calculations are carried out using a combinatorial method described in Ref. [7]. In both cases, realistic single-particle spectra and phenomenological collective enhancement of the level densities in deformed nuclei are used as input data. Because these calculations are carried out within the same model, and make use of the same single-particle and pairing strength parameters, a smooth joining of the discrete and continuous parts of the level densities is naturally achieved.

The semimicroscopic combined method mentioned above is very sensitive to the single-particle spectrum, in particular to levels close to the Fermi energy. Therefore, an accurate calculation of the single-particle states is necessary. Due to difficulties in calculating the single-particle spectrum for strongly deformed shapes, previous studies have generally employed methods appropriate to small deformations and extrapolated them to larger deformations. In this regard, and as part of our methodology, we have developed the code BARRIER [21], which calculates single-particle spectra in a deformed Woods-Saxon potential by using the Cassinian ovaloids proposed by Pashkevich to parameterize the nuclear shape [22]. Differently from the usual spherical-shape based Nilsson method for single-particle levels calculations, in the BARRIER code use is made of deformed shapes, and they are described by Cassinian ovals families, which contain the major part of the elongation associated with the dynamical fission process. Therefore, only deviations from ovaloid shapes are

estimated by expansion into series of Legendre polynomials. This procedure allows the building up of single-particle spectra by a more adequate calculation method for nuclear structures at large deformations.

#### IV. RESULTS AND DISCUSSION

Using the Strutinsky method with the Pashkevich parametrization of the nuclear shape, as introduced in the BARRIER code [21], we have calculated energy surface *vs.* deformation; the extreme points of the fission path were then determined. Furthermore, for the pairing strengths we considered  $G_N = 24.5 \text{ A}^{-1} \text{ MeV}$  and  $G_P = 27.5 \text{ A}^{-1} \text{ MeV}$  in all calculations. Thus, the single-particle spectra of  $^{237}\text{Np}$  at the deformation regions corresponding to the first saddle point of the fission barrier ( $\varepsilon = 0.369, \alpha_4 = -0.065$ ), the second well ( $\varepsilon = 0.502, \alpha_4 = 0.012$ ) and the second saddle ( $\varepsilon = 0.682, \alpha_3 = 0.107, \alpha_4 = 0.012$ ), were calculated. The parameter  $\varepsilon$  is associated with elongation and defines a concrete ovaloid base of Cassini family of figures, whereas  $\alpha_3$  and  $\alpha_4$  are linked to the deformation parameters of octupolar and hexadecapolar momenta, respectively, and are coefficients of the Legendre polynomials series expansion.

In Fig. 3 we show our calculated static fission barriers as functions of  $\varepsilon$  and  $\alpha_4$ , and with three different formulations for the macroscopic part [22–24]. As shown, the deformation coordinates are insensitive to the adopted macroscopic model, which only changes the relative height of the saddle points. This finding is additional evidence that our semimicroscopic approach, by considering with details the shell structure of hyperdeformed nuclear shapes, is able to explain the physical features related to fission cross-section structures of  $^{237}\text{Np}$ . In all cases, the second saddle point ( $B_B$ ) is higher than the first ( $B_A$ ) if we consider axial and mass symmetry along the fission path. This situation is inverted when we considered a more realistic mass asymmetry in the second saddle region via the inclusion of octupolar momentum in the calculation of the fission barrier. In Table I are reported the calculated barrier heights  $B_A$  and  $B_B$  for the three macroscopic formulations.

Our results for the first and second saddle points are presented in Table II and Fig. 1, where only the  $(J, \pi K)$  levels populated by  $E1$ ,  $M1$ , and  $E2$  transitions are shown for photon energies  $\omega < B_n$ . The height of the first saddle ( $A$ ), which is the higher of the two  $^{237}\text{Np}$  barriers, was considered equal to 5.6 MeV, as suggested by the substantial anisotropy of the  $^{237}\text{Np}$  photofission angular distribution measured elsewhere at  $\omega = 5.6 \text{ MeV}$  [25]. The suggested height for the second and

TABLE I. Fission barrier heights for  $^{237}\text{Np}$  at relevant points of the fission path calculated with the BARRIER code for different macroscopic parametrizations. S and MA stand for symmetric and asymmetric mass at the second saddle point, respectively.

Barrier height (MeV)	Ref. [22]	Ref. [23]	Ref. [24]
$B_A$	5.85	6.32	6.09
$B_B$ [S]	8.17	10.27	9.20
$B_B$ [MA]	3.99	6.22	5.14

TABLE II. Level scheme at the first (*A*) and second (*B*) saddle points of  $^{237}\text{Np}$ .

Barrier A, $B_A = 5.6$ MeV				Barrier B, $B_B = 5.2$ MeV			
$E$ (MeV)	$\pi K$	$J$	$\lambda L$	$E$ (MeV)	$\pi K$	$J$	$\lambda L$
0.0115	-1/2	3/2	$E1$	0.0000	1/2	1/2	$E2$
0.0128	5/2	5/2	$E2, M1$	0.0192	-1/2	3/2	$E1$
0.0139	7/2	7/2	$E2, M1$	0.0192	1/2	3/2	$E2, M1$
0.0322	-1/2	5/2	$E1$	0.0537	-1/2	5/2	$E1$
0.0469	5/2	7/2	$E2, M1$	0.0537	1/2	5/2	$E2, M1$
0.0536	-1/2	7/2	$E1$	0.0720	-3/2	3/2	$E1$
0.0588	7/2	9/2	$E2$	0.0720	3/2	3/2	$E2, M1$
0.0793	5/2	9/2	$E2$	0.0894	-1/2	7/2	$E1$
0.3885	1/2	1/2	$E2$	0.0894	1/2	7/2	$E2, M1$
0.4000	1/2	3/2	$E2, M1$	0.1110	-3/2	5/2	$E1$
0.4207	1/2	5/2	$E2, M1$	0.1110	3/2	5/2	$E2, M1$
0.4421	1/2	7/2	$E2, M1$	0.1515	1/2	9/2	$E2$
0.4793	1/2	9/2	$E2$	0.1530	-3/2	7/2	$E1$
0.6196	9/2	9/2	$E2$	0.1530	3/2	7/2	$E2, M1$
0.6531	-3/2	3/2	$E1$	0.2070	3/2	9/2	$E2$
0.6646	-1/2	3/2	$E1$	0.2910	-5/2	5/2	$E1$
0.6764	-3/2	5/2	$E1$	0.2910	5/2	5/2	$E2, M1$
0.6853	-1/2	5/2	$E1$	0.3165	-5/2	5/2	$E1$
0.7016	-3/2	7/2	$E1$	0.3165	5/2	5/2	$E2, M1$
0.7067	-1/2	7/2	$E1$	0.3165	-7/2	7/2	$E1$
0.7495	-3/2	3/2	$E1$	0.3165	7/2	7/2	$E2, M1$
0.7728	-3/2	5/2	$E1$	0.3165	-3/2	3/2	$E1$
0.7980	-3/2	7/2	$E1$	0.3165	3/2	3/2	$E2, M1$

lower saddle (*B*) is 5.2 MeV [11]. It is important to remark that the general behavior of the barrier heights obtained by the BARRIER code is similar to those obtained when using the LDM parameterization proposed in Refs. [22,24].

Before commenting on our results, we would like to add a few more arguments on the barrier heights and transition levels issues. Actually, we must take into account two key circumstances. (i) In the first place, there are several works presenting calculations of fission barrier heights, using semimicroscopic models based on the Strutinsky [26–28] and Hartree-Fock [29,30] methods. However, absolute values for barrier heights from these theoretical approaches, are systematically lower than those obtained from the fitting of cross sections by means of statistical model calculations [11–16,23,24]. (ii) In the second place, and considering that the uncertainties associated with our measurements [15] are modest, we note that small differences between the selected barrier heights entering our model calculations could eventually destroy the agreement between level groups (and level voids) and the corresponding structures in the measured cross sections. In fact, this drawback explains why theoretically obtained fission barriers are not generally used in statistical calculations of cross sections. Moreover, level densities at all the extreme points of the fission path are estimated from phenomenological formula [11–15].

In our approach, however, calculations of observable cross sections are performed with the aid of the fission barrier heights systematic [11,23]. Level spectra and level densities at the extreme points are calculated from single-particle spectra,

using available deformation parameters for the extreme points of the energy surface.

We observe the following distinct features associated with our calculations:

(i) The levels associated with the saddle point *A* are mostly grouped in the energy intervals 5.6–5.7 MeV, 6.0–6.1 MeV, and 6.2–6.35 MeV. These are rotational levels and the band heads are quasiparticle levels.

(ii) The agreement among these groups of levels and the experimentally observed ( $\gamma, f$ ) cross-section structures is very good.

(iii) The previously nonconclusive experimental evidences [4] for a subbarrier *A* structure around 5.2–5.3 MeV is now interpreted as arising from a group of levels at the top of saddle *B*.

(iv) The levels at 6.0–6.1 MeV, all of them with positive parity, are very likely populated by means of  $M1$  transitions, as indicated by a concentration of  $M1$  strength in  $^{237}\text{Np}$  around 6.2 MeV reported elsewhere [31]. Our calculations exclude the  $E1$  excitation nature of the structure around 6.0 MeV.

(v) The Bremsstrahlung derived ( $\gamma, f$ ) results for  $^{237}\text{Np}$  [10,12], where the energy resolution is poorer, exhibit a broad structure around 5.6–6.0 MeV. This could likely be the well-known energy resolution short coming associated with Bremsstrahlung beams, which manifests in this case as an inability to resolve structures around 5.7 and 5.95 MeV (see Fig. 4).

(vi) Also shown in Fig. 2 our result for the cross section, calculated from the present transition levels and transmission

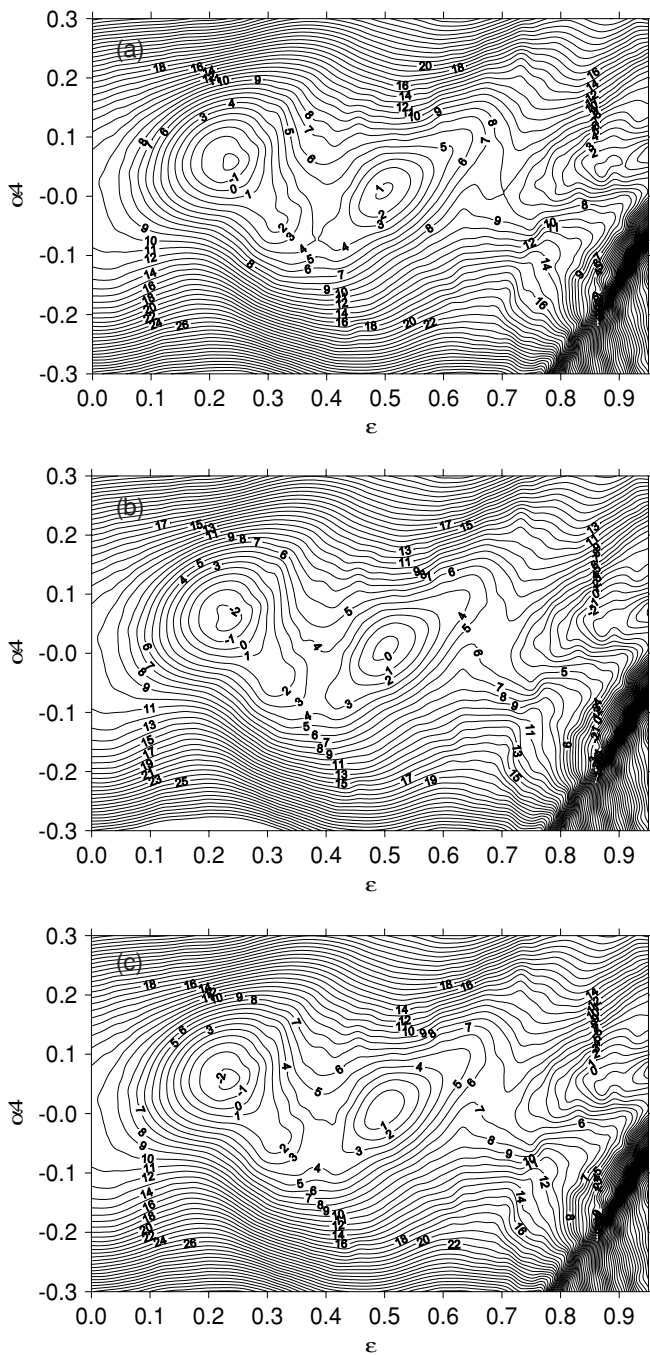


FIG. 3. Calculated fission barrier surfaces as functions of the  $\varepsilon$  and  $\alpha_4$  parameters, and for three different macroscopic formulations (a) from Ref. [22], (b) from Ref. [23], and (c) from Ref. [24]. The contour line separation is 1 MeV.

factors from the methodology and procedures developed by us recently [17]. The agreement with experimental data is good.

In addition, the calculations presented here represent a suitable tool to access information below the inner fission barrier  $B_A$ , because for this region all very important information coming from angular distributions is simply lost in the tunneling process. A totally different situation is verified for even-even actinides, where the detection and identifica-

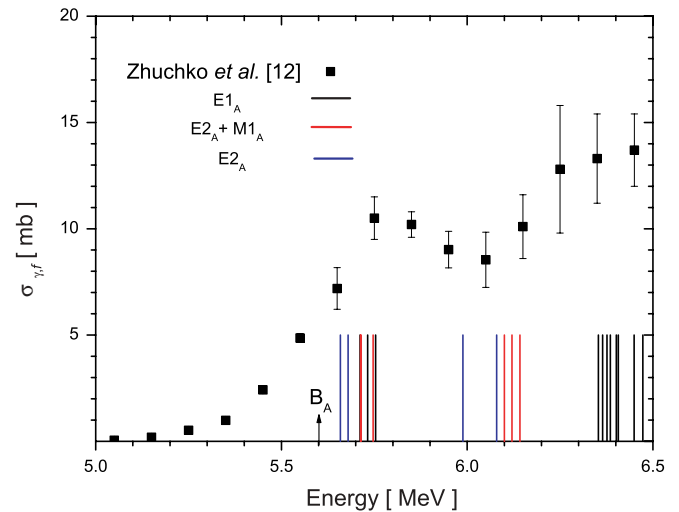


FIG. 4. (Color online) Photofission cross section of  $^{237}\text{Np}$  derived from Bremsstrahlung measurements [12], together with the calculated levels we obtained in this work at the top of the inner barrier, taking  $B_A = 5.6$  MeV.

tion of, e.g., isomeric fission, following the population of quasistationary levels of the second well, have been systematically carried out by means of both angular distributions and cross section measurements. This is clearly illustrated by photo- and electrofission studies performed in  $^{238}\text{U}$  [12] and  $^{232}\text{Th}$  [32], whereas more recent and complete cases could be appraised in Refs. [4] and [5] and references therein.

In summary, the above calculations (i) show that the structures experimentally observed in the  $^{237}\text{Np}(\gamma, f)$  process below  $B_n$ , are very probably related to the transition-level clusters distributed at the first and second saddle points. Such level distributions are dominated by their rotational nature. Therefore, the experimental observation of these structures is not an “unexpected” finding, as pointed out elsewhere [10]; (ii) put in evidence the angular momenta selectivity in a photoreaction, which generates a modulation in the transition levels spectra (alternating compression and rarefaction of levels). With hadronic probes, on the contrary, a plethora of uniformly distributed transition levels shows up and, therefore, no structure is observed in low-energy fission cross section, as, e.g., in the reaction  $^{236}\text{U}(^3\text{He}, df)$  [8,9]. Thus, the argument presented by Soldatov *et al.* [10] to rule out the fission nature of the 5.7- to 5.8-MeV structure in  $^{237}\text{Np}$  (see above) should not be valid at all; (iii) suggest that the Bremsstrahlung derived wide structure at 5.6–6.0 MeV [10] is in fact two unresolved sharper structures, also supported by higher resolution data [15]—see Figs. 2 and 4; and (iv) strongly suggest, finally, that the “5.5 MeV anomaly” invoked elsewhere [10] is pointless in the present case of  $^{237}\text{Np}(\gamma, f)$ , not to mention the lack of evidences regarding its manifestation in the actinide nuclei region.

## V. FINAL REMARKS

By solving a long-standing photofission problem, the case study presented in this article points to the opening of a new

investigation line for odd-actinides, where angular distributions are very difficult to be measured, by the combination of high energy resolution fission cross-section data with complete and detailed calculations of level distributions, particularly at large nuclear deformation regimes. Also, the approach here presented and applied for  $^{237}\text{Np}$  could be adapted for the study of many other fissionlike phenomena linked to single-particle peculiarities. We refer the reader, in this regard, to our previous study on second-well spectroscopy of  $^{237,239,241}\text{Pu}$  [3] and the neutron-induced fission process in  $^{233}\text{Pa}$  [17].

Calculations for well-deformed systems are quite actual, as, e.g., those performed by Ferreira and Maglione [33] for odd-odd deformed proton emitters, also a long-standing unsolved problem, which could be reproduced from our

approach not only for equilibrium deformations, but even for much larger deformations. Actually, we could extend the calculations up to the region of superheavy nuclei, because any kind of deformation could be considered in our approach. Shell effects should be present in these nuclei, originating structures associated with the saddle point, barrier minima, etc., and are the most likely characteristics responsible for fission decay peculiarities.

#### ACKNOWLEDGMENTS

Partially supported by FAPESP and CNPq, Brazilian agencies.

- 
- [1] A. Krasznahorkay, M. Hunyadi, M. N. Harakeh, M. Csatlos, T. Faestermann, A. Gollwitzer, G. Graw, J. Gulyas, D. Habs, R. Hertenberger, H. J. Maier, Z. Mate, D. Rudolph, P. Thierolf, J. Timar, and B. D. Valnion, *Phys. Rev. Lett.* **80**, 2073 (1998).
- [2] J. D. T. Arruda-Neto, M.-L. Yoneama, J. F. Dias, F. Garcia, M. A. V. Reigota, V. P. Likhachev, F. Guzmán, O. Rodríguez, and J. Mesa, *Phys. Rev. C* **55**, 2471 (1997).
- [3] F. Garcia, E. Garrote, M.-L. Yoneama, J. D. T. Arruda-Neto, J. Mesa, F. Bringas, J. F. Dias, V. P. Likhachev, O. Rodríguez, and F. Guzmán, *Eur. Phys. J. A* **6**, 49 (1999).
- [4] C. Wagemans, *The Nuclear Fission Process* (CRC Press, Boca Raton, 1991).
- [5] M.-L. Yoneama, E. Jacobs, J. D. T. Arruda-Neto, B. S. Bhandari, D. De Frenne, S. Pomme, K. Persyn, and K. Govaert, *Nucl. Phys.* **A604**, 263 (1996).
- [6] A. S. Soldatov, M. Y. Tsipenyuk, and G. N. Smirenkin, *Sov. J. Nucl. Phys.* **11**, 552 (1970) [*Yad. Fiz.* **11**, 992 (1970)].
- [7] S. A. Egorov, V. A. Rubchenya, and S. V. Khlebnikov, *Nucl. Phys.* **A494**, 75 (1989).
- [8] A. Gavron, H. C. Britt, E. Konecny, J. Weber, and J. B. Wilhelmy, *Phys. Rev. C* **13**, 2374 (1976).
- [9] H. C. Britt, *Physics and Chemistry of Fission* (IAEA, Vienna, 1980), Vol. 1, p. 3.
- [10] A. S. Soldatov, V. E. Rudnikov, G. N. Smirenkin, V. M. Andriyanov, V. A. Pilipchenko, and I. V. Khimich, *Phys. At. Nucl.* **56**, 1307 (1993) [*Yad. Fiz.* **56** (10), 16 (1993)].
- [11] S. Björnholm and J. E. Lynn, *Rev. Mod. Phys.* **52**, 725 (1980).
- [12] V. E. Zhuchko, Y. B. Ostapenko, G. N. Smirenkin, A. S. Soldatov, and Y. M. Tsipenyuk, *Sov. J. Nucl. Phys.* **28**, 611 (1978) [*Yad. Fiz.* **28**, 1185 (1978)].
- [13] Yu. B. Ostapenko, G. N. Smirenkin, A. S. Soldatov, and Yu. M. Tsipenyuk, *Sov. J. Part. Nucl.* **12**, 545 (1981) [*Fizika Elementarnykh Chastis I Atmnoyo Yadra* **2** (6), 1364 (1981)].
- [14] G. A. Bartholomew, E. D. Earle, A. J. Ferguson, J. W. Knowles, and M. A. Lone, *Adv. Nucl. Phys.* **7**, 229 (1973).
- [15] L. P. Geraldo, R. Semmler, O. L. Gonçalves, J. Mesa, J. D. T. Arruda-Neto, F. Garcia, and O. Rodríguez, *Nucl. Sci. Eng.* **136**, 357 (2000).
- [16] B. L. Berman, J. T. Caldwell, E. J. Dowdy, S. S. Dietrich, P. Meyer, and R. A. Alvarez, *Phys. Rev. C* **34**, 2201 (1986).
- [17] J. Mesa, J. D. T. Arruda-Neto, A. Deppman, V. P. Likhachev, M. V. Manso, C. E. Garcia, O. Rodríguez, F. Guzman, and F. Garcia, *Phys. Rev. C* **68**, 054608 (2003).
- [18] F. Garcia, O. Rodríguez, E. Garrote, and E. Lopez, *J. Phys. G* **19**, 2157 (1993).
- [19] F. Garcia, O. Rodríguez, V. A. Rubchenya, and E. Garrote, *Comput. Phys. Commun.* **86**, 129 (1995).
- [20] P. Decowski, W. Grochuls, A. Marcinko, K. Siwek, and Z. Wilhelmi, *Nucl. Phys.* **A110**, 129 (1968).
- [21] F. Garcia, O. Rodríguez, J. Mesa, J. D. T. Arruda-Neto, V. P. Likhachev, E. Garrote, R. Capote, and F. Guzmán, *Comput. Phys. Commun.* **120**, 57 (1999).
- [22] V. V. Pashkevich, *Nucl. Phys.* **A169**, 275 (1971).
- [23] M. Brack, J. Damgaard, A. S. Jensen, H. C. Pauli, V. M. Strutinsky, and C. Y. Wong, *Rev. Mod. Phys.* **44**, 320 (1972).
- [24] H. C. Pauli and T. Ledergerber, *Phys. Lett.* **B34**, 264 (1971).
- [25] L. P. Geraldo, *J. Phys. G* **12**, 1423 (1986).
- [26] P. Moller, J. R. Nix, and W. Swiatecki, *Nucl. Phys.* **A492**, 349 (1989).
- [27] S. Cwiok and A. Sobiczewski, *Z. Phys. A* **342**, 203 (1992).
- [28] W. D. Myers and W. J. Swiatecki, *Acta Phys. Pol. B* **28**, 9 (1997).
- [29] J. F. Berger, M. Girod, and D. Gogny, Paper presented at the Conference "50 years with Nuclear Fission," Washintong D.C. and Gaithersburg, MD, April 25–28, 1989.
- [30] M. Bender, K. Rutz, P.-G. Reinhard, A. Maruhn, and W. Greiner, *Phys. Rev. C* **58**, 2126 (1998).
- [31] J. D. T. Arruda-Neto, S. L. Paschoal, and S. B. Herdade, *J. Phys. G* **14**, 373 (1988).
- [32] J. D. T. Arruda-Neto, E. Jacobs, D. De Frenne, and S. Pomme, *Phys. Lett.* **B248**, 34 (1990).
- [33] L. S. Ferreira and E. Maglione, *Phys. Rev. Lett.* **86**, 1721 (2001).